



# Development and characterization of alginate@montmorillonite hybrid microcapsules for encapsulation and controlled release of quercetin: Effect of clay type

Kamal Essifi <sup>a,\*</sup>, Mohamed Brahmi <sup>a</sup>, Doha Berraouan <sup>a</sup>, Amina Amrani <sup>a</sup>, Ali El Bachiri <sup>a</sup>, Marie Laure Fauconnier <sup>b</sup>, Abdesselam Tahani <sup>a</sup>

<sup>a</sup> Physical Chemistry of Natural Resources and Process Team, Laboratory of Applied Chemistry and Environment (CPSUNAP-LCAE), Department of Chemistry, Faculty of Sciences, Mohammed First University, Oujda, Morocco

<sup>b</sup> Laboratory of Chemistry of natural molecules, Gembloux Agro-Bio Tech, University of Liège, Belgium

## ARTICLE INFO

### Article history:

Available online 28 July 2022

### Keywords:

Alginate microcapsules  
Quercetin  
Montmorillonite  
Hybrid microcapsules  
Encapsulation  
Controlled release

## ABSTRACT

In the present study, different organic and hybrid systems for quercetin (Qr) encapsulation were developed, namely Ca-Alginate (Qr-Alg), Ca-Alginate@Na-montmorillonite (Qr-Alg@Na-Mnt), and Ca-Alginate@CPC-montmorillonite (Qr-Alg@CPC-Mnt).

Attenuated total reflecting-Fourier-transform infrared (ATR-FTIR) analysis was used to characterize and prove quercetin encapsulation in the developed microcapsules. The encapsulation efficiency (EE) and loading capacity (LC) of quercetin in elaborated biomaterials were determined. Besides, the release kinetics of quercetin molecules from organic and hybrid microcapsules were carefully investigated in two different aqueous mediums; pure distilled water and distilled water containing Tween 20 (1%, w/v).

The obtained results show that all developed microcapsules have a good encapsulation efficiency and loading capacity within the range  $97.65 \pm 0.57$ – $99.47 \pm 0.38\%$  for the EE and  $19.26 \pm 0.46$ – $23.29 \pm 0.82$  mg/g for the LC. The release rates of Qr from organic microcapsules Qr-Alg, hybrid microcapsules Qr-Alg@Na-Mnt, and Qr-Alg@CPC-Mnt in distilled water containing Tween 20 (1%, w/v) are 52, 49, and 113 times bigger, respectively, than release rate in distilled water.

In addition, the kinetics release from hybrid microcapsules was slower in comparison to organic microcapsules. Also, in the case of hybrid microcapsules, the rate of kinetic release of quercetin from Qr-Alg@Na-Mnt was greater than the one from Qr-Alg@CPC-Mnt. This is due to the strong interactions of quercetin molecules with nanoparticle functional groups of cetylpyridinium chloride modified montmorillonite organoclay (CPC-Mnt) compared to sodium montmorillonite (Na-Mnt). The kinetics of Quercetin release from all developed organic and hybrid microcapsules follows the Korsmeyer-Peppas model and is controlled by non-Fickian diffusion.

Copyright © 2023 Elsevier Ltd. All rights reserved.

Selection and peer-review under responsibility of the scientific committee of the Fifth edition of the International Conference on Materials & Environmental Science.

## 1. Introduction

Quercetin (3,3',4',5,7-pentahydroxyflavone), a bioactive substance and a typical flavonol-type flavonoid, exists generally in a variety of vegetables, fruit, and grains [1–3]. Quercetin has attracted considerable attention by researchers, due to its beneficial and promising application in the pharmaceutical field considering its activities as anti-cancer [4,5], antidiabetic [6], antiviral

[7,8], anti-inflammatory [9,10], and antibacterial [11,12], and also as an antioxidant of oils [13].

On the other hand, the short half-life [14], the low water solubility [15], and the low oral bioavailability of quercetin [16] make it an exceptional candidate to research technological solutions to improve its chemical stability, bioaccessibility, and ensure the goal of slow-release for taking advantage of its powerful therapeutic benefits [17].

Microencapsulation technology is a widely used and very effective way to protect bioactive substances. It can improve the stability of the encapsulated component from external harsh conditions

\* Corresponding author.

E-mail address: [kamal.essifi.lpapc@gmail.com](mailto:kamal.essifi.lpapc@gmail.com) (K. Essifi).

in final products and during processing, masking the undesirable odors and tastes of ingredients, and helps with the deliverance of the encapsulated matter at controlled rates, at a certain time, and in a certain place [18,19]. The choice of shell material is an important step when encapsulating a bioactive substance, generally, the physicochemical and mechanical characteristics of a microcapsule are directly linked to this shell. Additionally, these structural properties are easily affected by the structure and the thickness of the wall material, the chemical composition, and the size of the microcapsule [18,20].

Although different materials for preparing microcapsules have been investigated, the organic and hybrid microparticles based on sodium alginate biopolymer, and alginate/clay are the most widely used due to their bioadhesive, biocompatible, biodegradable, and bioavailability [3,21–23].

Alginate acid extracted from brown algae is a natural polysaccharide that has many advantages compared to commonly used biopolymers for hydrogel beads formulation [24]. The mannuronic acid (M–block), gluconic acid (G–block), and mixed sequences of M–G–blocks are the main chains that constitute the alginate polymer. The sequence and ratio (M/G) of these uronic acids vary with the origin of alginate and can determine its properties [25]. As a result of the biocompatibility, biodegradability, low cost, and a non-toxicity of such biomaterial and its gelling properties when crosslinked with divalent ions such as  $\text{Ca}^{2+}$ ,  $\text{Ba}^{2+}$ , and  $\text{Fe}^{2+}$  cations, a broad range of applications can be found in food and pharmaceutical industries as hydrogel encapsulation system [20,26–30].

Clay mineral–polymer hybrid microcapsules are a highly intriguing option for modifying bioactive substance release. Although clay minerals and polymers were commonly utilized as single bioactive substance carriers in their pure form, this type of material did not always satisfy all of the requirements. The development of polymer-layered silicate hybrid materials provided the opportunity to improve the characteristics of each component individually [31–33].

The kinetics release and the release rate of bioactive substances depend on several factors including the structure of these compounds, their solubility in the phases inside the microparticles and the release medium, and their interactions with microparticles composition. Also, the physicochemical properties of the encapsulating material like the pore size, shape, particle size, and the concentration gradient of bioactive substance between the microcapsules wall and its surrounding environment [34–39].

As a contribution to a large number of researches on this matter, in the present study, we mainly focused on the encapsulation of quercetin as a flavonoid bioactive substance in calcium alginate organic microcapsules and alginate montmorillonite mineral clay hybrid microcapsules. Organic and hybrid encapsulation systems based on alginate polymer and two types of montmorillonite mineral clay, the sodium montmorillonite (Na-Mnt) and the cetylpyridinium chloride modified montmorillonite organoclay (CPC-Mnt) were developed to improve the chemical stability, the availability, and the controlled release of quercetin in an aqueous medium.

## 2. Materials and methods

### 2.1. Materials

Sodium alginate (alginic acid sodium salt from brown algae, #MKBZ4415V, medium viscosity, 5–40 cps of 1% aqueous solution) was purchased from Sigma-Aldrich Co. (St. Louis, USA). Quercetin (purity  $\geq 99\%$ ), Tri-sodium citrate, Tween 20, Dimethyl sulfoxide (DMSO), and Calcium Chloride dihydrate were provided by Sigma-Aldrich Co. (St. Louis, USA). Distilled water that was used for the preparation of all samples has conductivity less than  $2\mu\text{S}$ .

The montmorillonite used in this study is a natural clay from Nador (North-East of Morocco) that was purified and modified by  $\text{Na}^+$  (Na-Mnt) and cetylpyridinium chloride (CPC) surfactant (CPC-Mnt) according to the methods already described in our previous papers [40,41].

### 2.2. Preparing organic and hybrid microcapsules

Calcium alginate organic microcapsules and calcium alginate@montmorillonite hybrid microcapsules containing quercetin were prepared using the ionotropic gelation method as described previously in our works [26] with some modifications. Briefly, for calcium alginate organic microcapsules, sodium alginate solution with a 3% (w/v) concentration was prepared by dissolving 0.75 g of alginate polymer in 23 ml of distilled water at 900 rpm at room temperature. Meanwhile, a quercetin solution was made by dissolving 0.2 g of quercetin in 8 ml DMSO. Then, 2 ml of the quercetin solution were added to the sodium alginate solution (23 ml) under magnetic stirring until a homogenized final solution formed.

For calcium alginate@montmorillonite hybrid microcapsules, a suspension with 1% (w/v) of Na-montmorillonite (Na-Mnt) or CPC-montmorillonite (CPC-Mnt) was prepared by dispersing 0.25 g of clay in 23 ml of distilled water at 900 rpm at room temperature. After total dispersion of clay nanoparticles, 2 ml of the quercetin solution were added to the clay suspension (23 ml) under magnetic stirring until a homogenized final solution formed. Then, 0.75 g of alginate polymer was added to the mixture of quercetin and montmorillonite clay (25 ml) under magnetic stirring until a homogenized final solution formed. The final homogenized solutions were left to stand to remove air bubbles from the aqueous medium.

The gelling-bath solution was prepared by dissolving  $\text{CaCl}_2$  in distilled water at 4% (w/v). A pump was applied to control the delivery of the mixed solutions through a tube that was connected with a polypropylene micropipette tip, the mixture solutions fall into the  $\text{CaCl}_2$  solution continuously.

## 3. Characterization techniques

### 3.1. Loading capacity (LC) and encapsulation efficiency (EE) of quercetin in organic and hybrid microcapsules

The amount of quercetin ( $Q_r$ ) was determined by the direct measurement of the absorbance using a UV-visible spectrophotometer at 376 nm. The concentration of  $Q_r$  was obtained through a calibration curve using  $Q_r$  as the standard reference under the same experimental conditions. Loading capacity was calculated using the following formula:

$$\text{Loading capacity (LC, g/g)} = \frac{\text{weight of } Q_r \text{ in the microcapsules (g)}}{\text{weight of dried microcapsules (g)}}$$

The encapsulation efficiency was calculated using the formula below:

$$\text{Encapsulation efficiency (EE, \%)} = \frac{\text{amount of } Q_r \text{ in the microcapsules}}{\text{initial amount of } Q_r} \times 100$$

### 3.2. Attenuated total reflecting-Fourier-transform infrared (ATR-FTIR) analysis

To evaluate and confirm the interaction between alginate microcapsules and quercetin molecules ( $Q_r$ ), the ATR-FTIR technique was used. The spectrums were carried out on a Jasco4700-

ATR spectrophotometer (Shimadzu, Japan), in the wavelength region between 400 and 4000  $\text{cm}^{-1}$ . Furthermore, each spectrum was obtained by averaging 32 scans at a resolution of 4  $\text{cm}^{-1}$ .

### 3.3. Morphological characterization

A digital camera was employed for imaging to estimate the morphology of the obtained organic and hybrid developed microcapsules.

### 3.4. Quercetin kinetics release

The release of quercetin molecules from the elaborated microparticles in a pure aqueous medium and an aqueous medium containing Tween 20 (1% w/v) using an amber-colored glass bottle was achieved using a UV–visible spectrophotometer. The analysis was realized based on our previously described method [26], briefly, a known amount of microcapsules was suspended in 100 ml of pure distilled water or distilled water containing Tween 20 (1% w/v). The samples underwent continuous agitation on a Multi-Position magnetic stirrer (Variomag Poly 15, Germany) operating at 250 rpm. At defined time intervals, an aliquot of the supernatant was taken for the measurement of the absorbance at 376 nm, and the released quercetin amount was obtained by using concentration versus absorbance calibration curves with and without Tween (1% w/v). Finally, 30 ml of a sodium citrate solution (2%, w/v) were added and final absorbance was recorded and corrected by considering the dilution.

### 3.5. Determination of release kinetics of quercetin from organic and hybrids microcapsules

To determine release kinetic behavior for each developed organic and hybrid microcapsules, zero-order, first-order, and Korsmeyer-Peppas release models were studied (Table 1) [42,43].

$Q_t$ : Amount of the active compound released at time  $t$  (the release time),  $Q_0$ : initial value  $Q$ , whereas  $k_0$ : zero-order release constant,  $k_1$ : first-order release constant,  $k_p$ : Korsmeyer–Peppas release constant and  $n$  is the diffusional exponent, indicative of encapsulated compound release mechanism.

Using OriginPro 2018 software, the calculation of the squared correlation coefficient ( $R^2$ ) was used to confirm the accuracy of those models.

## 4. Results and discussions

### 4.1. Loading capacity (LC) and encapsulation efficiency (EE) of quercetin in organic and hybrid microcapsules

The obtained results of the encapsulation efficiency (EE) and the loading capacity (LC) for all elaborated organic and hybrid microcapsules such as Ca-Alginate (Qr-Alg), Ca-Alginate@Na-montmorillonite (Qr-Alg@Na-Mnt) and Ca-Alginate@CPC-montmorillonite (Qr-Alg@CPC-Mnt) are presented in Fig. 1. Considering the applied encapsulation method, the used polymer, the montmorillonite clay properties, and quercetin solubility in

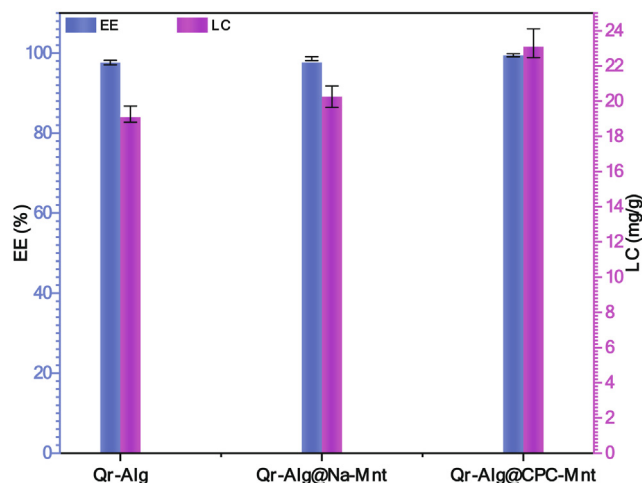


Fig. 1. Encapsulation Efficiency (EE) and Loading Capacity (LC) of Quercetin in Qr-Alg, Qr-Alg@Na-Mnt, and Qr-Alg@CPC-Mnt microcapsules.

water, the LC and EE values were satisfying. As shown in Fig. 1, all formulations show a higher EE, with the obtained values of EE of Qr in calcium alginate (Qr-Alg), calcium alginate@Na-montmorillonite (Qr-Alg@Na-Mnt), and calcium alginate@CPC-montmorillonite (Qr-Alg@CPC-Mnt) are 97.65 ± 0.57%, 98.62 ± 0.49%, and 99.47 ± 0.38% respectively. The higher EE is due to the lower solubility of quercetin in water.

In addition, the loading capacity and encapsulation efficiency are influenced by the incorporation of montmorillonite clay nanoparticles and also, the clay type. Whereas, the LC values of Qr in organics microcapsules (Qr-Alg), and hybrid microcapsules (Qr-Alg@Na-Mnt) and (Qr-Alg@CPC-Mnt) are 19.26 ± 0.46, 20.25 ± 0.61, and 23.29 ± 0.82 (mg/g) respectively. This indicates that, further to their barrier role, montmorillonite nanoparticles are the encapsulation system for quercetin molecules.

Zulay Gabriela Cadena-Velandia et al. [3] mentioned that the loading capacity and encapsulation efficiency of quercetin in alginate microparticles are 1.43% ± 0.01 w/w, and 96.21% ± 0.05% respectively. In other studies, the EE is lower than 94% [3,44,45]. Comparing our results with the reported study shows that our elaborated encapsulation systems have a great loading capacity for quercetin encapsulation.

### 4.2. Attenuated total reflecting-fourier-transform infrared (ATR-FTIR) analysis

ATR-FTIR spectra of quercetin (Qr), blank calcium alginate microcapsules (Ca-Alg), blank Ca-Alginate@Na-montmorillonite hybrid microcapsules (Ca-Alg@Na-Mnt), blank Ca-Alginate@CPC-montmorillonite hybrid microcapsules (Ca-Alg@Na-Mnt), calcium alginate microcapsules loaded quercetin (Qr-Alg), Ca-Alginate@Na-montmorillonite hybrid microcapsules loaded quercetin (Qr-Alg@Na-Mnt), and Ca-Alginate@CPC-montmorillonite hybrid microcapsules loaded quercetin (Qr-Alg@CPC-Mnt) are presented in Fig. 2.

The ATR-FTIR spectrum of quercetin (Qr) showed a broad peak at 3253.32  $\text{cm}^{-1}$  attributed to the stretching vibration of the phenolic OH group. The peak observed at 1660.41  $\text{cm}^{-1}$  is for aryl C = O stretching. The peaks at 1605.45  $\text{cm}^{-1}$ , 1509.99  $\text{cm}^{-1}$ , and 1461.78  $\text{cm}^{-1}$  are due to the aromatic stretching of C–C, C = O, and C = C respectively. The peaks at 1349.93  $\text{cm}^{-1}$  and 1312.32  $\text{cm}^{-1}$  are due to the bending of phenolic –OH and aromatic C–H. The peaks at 1239.04  $\text{cm}^{-1}$  and 1209.15  $\text{cm}^{-1}$  are due

Table 1  
Mathematical models used to describe the release kinetics of quercetin.

Model	Equation
Zero-order	$Q_t = k_0 t + Q_0$
First-order	$Q_t = Q_0 e^{k_1 t}$
Korsmeyer–Peppas	$Q_t = k_p t^n$

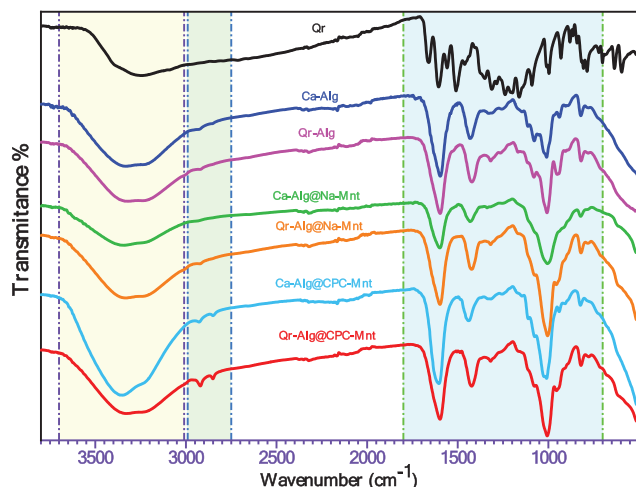


Fig. 2. ATR-FTIR spectra of quercetin (Qr), blank microcapsules, and quercetin-loaded microcapsules.

to the stretching of aryl ether C–O and phenols C–O. A similar observation was observed by other authors [3,44–46].

For the blank calcium alginate microcapsules (Ca-Alg) a broad peak at  $3342\text{ cm}^{-1}$  was assigned to  $\text{H}_2\text{O}$  molecules. Additionally, for the two peaks of  $\text{COO}^-$  groups, a remarked shift toward higher wavenumber was observed ( $1598\text{ cm}^{-1}$  and  $1435\text{ cm}^{-1}$  for the symmetrical and asymmetrical vibrations respectively), suggesting that  $\text{Ca}^{2+}$  cross-linked the  $\text{COO}^-$  groups of the alginate.

The ATR-FTIR spectra of blank hybrid microcapsules (Ca-Alg@Na-Mnt) show that all the characteristic bands of the calcium alginate organic microcapsules have appeared. Therefore, it is inferred that sodium montmorillonite and calcium alginate act as a simple physical mixture. Moreover, in the case of the blank hybrid microcapsules (Ca-Alg@CPC-Mnt), two bands at  $2927.41$  and  $2851.24\text{ cm}^{-1}$  attributed to the stretching vibration of the alkyl  $\text{CH}_2$  chain of CPC have been observed.

The encapsulation of quercetin in organic and hybrid microcapsules shows the shifting of stretching vibration of the O–H group to the lower frequencies. Moreover, practically all peaks of the quercetin molecule and the composition of the microcapsules diminished or augmented in intensity, widened, or shifted. This observation indicates that there may be a hydrogen-bonding interaction between the quercetin molecules and the functional groups of alginate and montmorillonite as reported in numerous previous papers [3,22,23,44–46].

#### 4.3. Morphological characterization

Fig. 3) presents the digital photos of blank calcium alginate organic microcapsules (Ca-Alg), blank Ca-Alginate@Na-montmorillonite hybrid microcapsules (Ca-Alg@Na-Mnt), blank Ca-Alginate@CPC-montmorillonite hybrid microcapsules (Ca-Alg@Na-Mnt), calcium alginate microcapsules loaded quercetin (Qr-Alg), Ca-Alginate@Na-montmorillonite hybrid microcapsules loaded quercetin (Qr-Alg@Na-Mnt), and Ca-Alginate@CPC-montmorillonite hybrid microcapsules loaded quercetin (Qr-Alg@CPC-Mnt).

The morphological characterization results show that all obtained organic and hybrid microcapsules have spherical and smooth surface textures with relatively uniform distribution sizes. By comparing the blank microcapsules photos with loaded ones, it is noticed the encapsulation of quercetin molecules. In addition, the LC and EE results show that the Qr-Alg@CPC-Mnt hybrid microcapsules have a higher EE and LC compared to the hybrid Qr-

Alg@Na-Mnt and organic Qr-Alg capsules, which is in agreement with the appeared color of quercetin-loaded microparticles.

#### 4.4. Quercetin kinetics release

Fig. 4) represents, the kinetics release of the quercetin from organic microcapsules the Qr-Alg and hybrid microcapsules the Qr-Alg@Na-Mnt, and the Qr-Alg@CPC-Mnt at  $25\text{ }^\circ\text{C}$  in distilled water (Fig. 4A) and in distilled water containing Tween 20 (1%, w/v) (Fig. 4B). The obtained results show that the release of Qr in distilled water was slower in comparison to distilled water containing Tween 20 (1%, w/v) for all microcapsules types. The restricted solubility of the quercetin molecules in the aqueous medium would be the reason.

For the release in distilled water (Fig. 4A), the cumulative release of quercetin was 1.68, 1.51, and 0.56% in 10 h from the organic microcapsules Qr-Alg and the hybrid microcapsules Qr-Alg@Na-Mnt, and Qr-Alg@CPC-Mnt respectively.

However, the cumulative release of quercetin in distilled water containing Tween 20 (1%, w/v) (Fig. 4B) was 87.67, 74.69, and 63.40% in 36 h, respectively, from the organic microcapsules Qr-Alg and the hybrid microcapsules Qr-Alg@Na-Mnt, and Qr-Alg@CPC-Mnt.

As is seen in Fig. 4, the structure and the composition of the microcapsules matrix showed a clear effect on the kinetics release of quercetin. The kinetics release from hybrid microcapsules was slower in comparison to organic microcapsules, also, in the case of hybrid microcapsules, the quercetin release from Qr-Alg@Na-Mnt was faster than the release of quercetin from Qr-Alg@CPC-Mnt, this trend can be explained by the high hydrophobicity of organoclay nanoparticles (CPC-Mnt) compared to sodium montmorillonite nanoparticles (Na-Mnt). This indicates that the quercetin molecules are in strong interactions with nanoparticle functional groups of CPC-Mnt compared to Na-Mnt.

The release results showed that the incorporation of montmorillonite nanoparticles in alginate microcapsules improved the controlled release of quercetin. Also, the release medium is a parameter to control the kinetics release of encapsulated substances.

#### 4.5. Determination of release kinetics of quercetin from organic and hybrids microcapsules

Based on the values of the correlation coefficients ( $R^2$ ) shown in Table 2, the release of quercetin from all developed microcapsules fits the Korsmeyer-Peppas model.

The Korsmeyer-Peppas model describes and determines the release mechanism of the encapsulated substance between three expected mechanisms, Fickian release (diffusion-controlled release), non-Fickian release (anomalous transport), and case-II transport (relaxation-controlled release) [43,47].

The use of the Korsmeyer-Peppas model requires the determination of exponent  $n$ , accordingly, it is suggested to use only the first 60% of the substance release data. The  $n$  value gives a clue about the type of the release mechanism, in which the Fickian release is verified at  $n$  value less than 0.43, while the non-Fickian release mechanism is established where  $n$  value is between 0.43 and 0.85, although the  $n$  value higher than 0.85 indicates the case-II transport release [43,47,48].

In all release mediums and for all elaborated encapsulation systems, the  $n$  values were between 0.43 and 0.85, which indicates that the quercetin mechanism release according to the non-Fickian diffusion. Meaning that during the quercetin release, sharp barriers are separating the highly swollen regions from the crystalline regions.

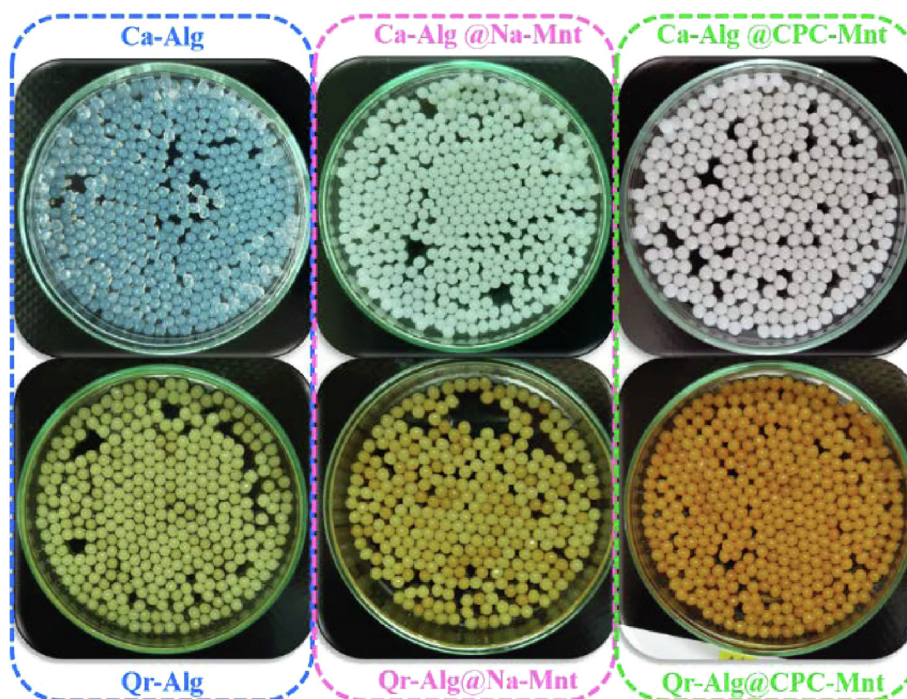


Fig. 3. Digital photos of blank microcapsules, and quercetin-loaded microcapsules.

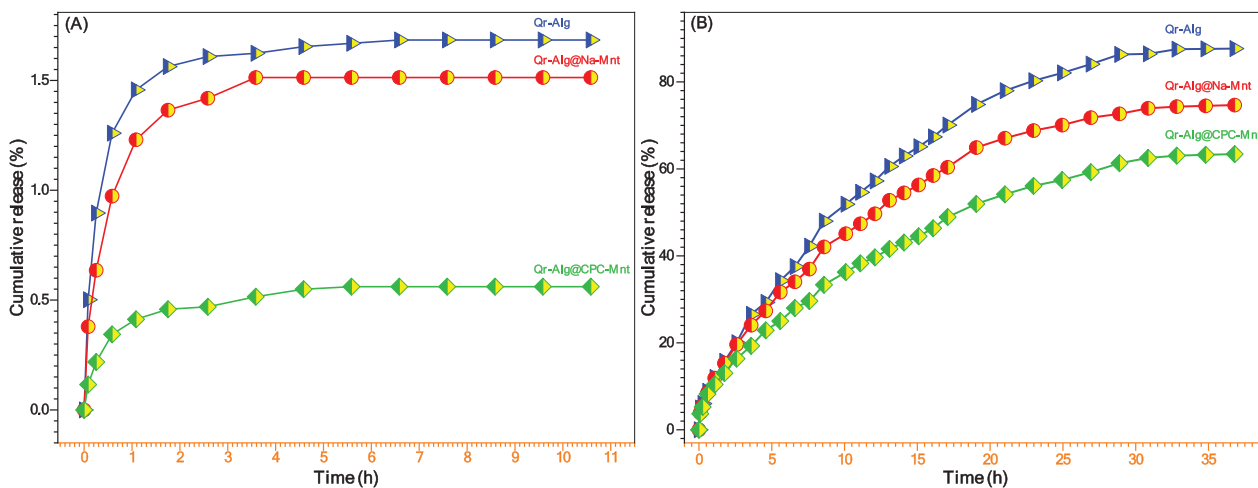


Fig. 4. Kinetics release of the quercetin from organic and hybrid microcapsules in (A) distilled water and (B) distilled water containing Tween 20 (1%, w/v).

Table 2  
The release kinetics parameters of quercetin for different models.

Microcapsules code	mathematical models						
	Zero-Order		First-Order		Korsmeyer-Peppas		
	<b>Release in pure distilled water</b>						
	<b>R<sup>2</sup></b>	<b>k<sub>0</sub></b>	<b>R<sup>2</sup></b>	<b>k<sub>1</sub></b>	<b>R<sup>2</sup></b>	<b>k<sub>p</sub></b>	<b>n</b>
Qr-Alg	0.9552	0.0678	0.8895	1.7244	0.9945	0.0166	0.4757
Qr-Alg@Na-Mnt	0.9876	0.0608	0.9408	1.7982	0.9996	0.0125	0.4836
Qr-Alg@CPC-Mnt	0.9825	0.0275	0.9202	2.0681	0.9995	0.0046	0.5624
	<b>Release in distilled water containing Tween 20 (1%, w/v)</b>						
	<b>R<sup>2</sup></b>	<b>k<sub>0</sub></b>	<b>R<sup>2</sup></b>	<b>k<sub>1</sub></b>	<b>R<sup>2</sup></b>	<b>k<sub>p</sub></b>	<b>n</b>
Qr-Alg	0.9864	0.1073	0.9142	0.3453	0.9910	0.1219	0.5541
Qr-Alg@Na-Mnt	0.9846	0.1113	0.8891	0.3371	0.9982	0.1163	0.5505
Qr-Alg@CPC-Mnt	0.9852	0.0763	0.8930	0.3021	0.9958	0.1035	0.4916

## 5. Conclusion

In summary, bioactive substance delivery systems based on the alginate polymer and two types of montmorillonite mineral clay, the sodium montmorillonite (Na-Mnt) and the cetylpyridinium chloride modified montmorillonite organoclay (CPC-Mnt) were successfully prepared by the ionotropic gelation method.

The ATR-FTIR result confirmed the incorporation of quercetin in the organic and hybrid microcapsules, with a possibility of its interaction with the composition of the microparticles. The obtained microcapsules appeared spherical with smooth surface texture and relatively uniform distribution sizes.

The loading capacity (LC) and encapsulation efficiency (EE) were found to be influenced by the incorporation of montmorillonite mineral clay nanoparticles and also, by the nature of the clay type.

The release kinetics of quercetin as flavonoid bioactive substance loaded organic and hybrid microcapsules were studied in distilled water and distilled water containing Tween 20 (1%, w/v). The obtained result showed that the release of Qr in distilled water was slower in comparison to the release in distilled water containing Tween 20 (1%, w/v) for all developed microcapsules.

On the other hand, the kinetics release from hybrid microcapsules was slower in comparison to organic microcapsules, also, in the case of hybrid microcapsules, the quercetin release from Qr-Alg@Na-Mnt was faster than the release of quercetin from Qr-Alg@CPC-Mnt. This indicates that the quercetin molecules are in strong interactions with nanoparticle functional groups of CPC-Mnt compared to Na-Mnt. The kinetics of Quercetin release from all developed organic and hybrid microcapsules follows the Korsmeyer–Peppas model and is controlled by non-Fickian diffusion.

The findings indicate that the developed hybrid microcapsules based on alginate polymer and sodium montmorillonite (Na-Mnt) or cetylpyridinium chloride modified montmorillonite organoclay (CPC-Mnt) are promising systems to encapsulate and control the release of water-insoluble flavonoid compounds such as quercetin to further increase their applications in functional formulations.

## CRedit authorship contribution statement

**Kamal Essifi:** Formal analysis, Investigation, Writing – original draft. **Mohamed Brahmi:** Formal analysis, Software, Supervision. **Doha Berraouan:** Formal analysis, Supervision. **Amina Amrani:** Formal analysis, Supervision. **Ali El Bachiri:** Validation, Data curation, Supervision. **Marie Laure Fauconnier:** Validation, Data curation, Supervision. **Abdesselam Tahani:** Conceptualization, Resources, Writing – review & editing, Supervision, Project administration, Funding acquisition.

## Data availability

No data was used for the research described in the article.

## Declaration of Competing Interest

The authors declare that they have no known competing financial interests or personal relationships that could have appeared to influence the work reported in this paper.

## Acknowledgments

The authors are sincerely thankful to MESRSFC, CNRST-Morocco, and UMP for their financial support of Project PPR 15-17 and PARA1-2019. The authors are also thankful to Professor

Abdelmonaem Talhaoui, Head of the Department of Chemistry, Faculty of Sciences, Mohammed First University, Oujda, Morocco, for managing the Department of analysis.

## References

- [1] E. Van Hecke, M. Benali, Solid dispersions of quercetin-PEG matrices: miscibility prediction, preparation and characterization, *Food Biosci.* 49 (2022), <https://doi.org/10.1016/j.fbio.2022.101868>.
- [2] L. Huang, M. Li, H. Wei, Q. Yu, S. Huang, T. Wang, M. Liu, P. Li, Research on the indirect antiviral function of medicinal plant ingredient quercetin against grouper iridovirus infection, *Fish Shellfish Immunol.* 124 (2022) 372–379, <https://doi.org/10.1016/j.fsi.2022.04.013>.
- [3] Z.G. Cadena-Velandia, J.C. Montenegro-Alarcón, X. Marquín-Casas, C.E. Mora-Huertas, Quercetin-loaded alginate microparticles: a contribution on the particle structure, *J. Drug Delivery Sci. Technol.* 56 (2020), <https://doi.org/10.1016/j.jddst.2020.101558>.
- [4] Z.H. Shi, N.G. Li, Y.P. Tang, Q.P. Shi, W. Zhang, P.X. Zhang, Z.X. Dong, W. Li, X. Zhang, H.A. Fu, J.A. Duan, Synthesis, biological evaluation and SAR analysis of O-alkylated analogs of quercetin for anticancer, *Bioorg. Med. Chem. Lett.* 24 (2014) 4424–4427, <https://doi.org/10.1016/j.bmcl.2014.08.006>.
- [5] P. Wang, K. Zhang, Q. Zhang, J. Mei, C.J. Chen, Z.Z. Feng, D.H. Yu, Effects of quercetin on the apoptosis of the human gastric carcinoma cells, *Toxicol. In Vitro* 26 (2012) 221–228, <https://doi.org/10.1016/j.tiv.2011.11.015>.
- [6] P. Mukhopadhyay, S. Maity, S. Mandal, A.S. Chakraborti, A.K. Prajapati, P.P. Kundu, Preparation, characterization and in vivo evaluation of pH sensitive, safe quercetin-succinylated chitosan-alginate core-shell-corona nanoparticle for diabetes treatment, *Carbohydr. Polym.* 182 (2018) 42–51, <https://doi.org/10.1016/j.carbpol.2017.10.098>.
- [7] H.J. Choi, J.H. Song, K.S. Park, D.H. Kwon, Inhibitory effects of quercetin 3-rhamnoside on influenza A virus replication, *Eur. J. Pharm. Sci.* 37 (2009) 329–333, <https://doi.org/10.1016/j.ejps.2009.03.002>.
- [8] M. Thapa, Y. Kim, J. Desper, K.O. Chang, D.H. Hua, Synthesis and antiviral activity of substituted quercetins, *Bioorg. Med. Chem. Lett.* 22 (2012) 353–356, <https://doi.org/10.1016/j.bmcl.2011.10.119>.
- [9] D. Fan, X. Zhou, C. Zhao, H. Chen, Y. Zhao, X. Gong, Anti-inflammatory, antiviral and quantitative study of quercetin-3-O-β-D-glucuronide in Polygonum perfoliatum L., *Fitoterapia* 82 (2011) 805–810, <https://doi.org/10.1016/j.fitote.2011.04.007>.
- [10] R. Kleemann, L. Verschuren, M. Morrison, S. Zedelaar, M.J. van Erk, P.Y. Wielinga, T. Kooistra, Anti-inflammatory, anti-proliferative and anti-atherosclerotic effects of quercetin in human in vitro and in vivo models, *Atherosclerosis* 218 (2011) 44–52, <https://doi.org/10.1016/j.atherosclerosis.2011.04.023>.
- [11] R. Paolillo, C. Romano Carratelli, A. Rizzo, Effect of resveratrol and quercetin in experimental infection by Salmonella enterica serovar Typhimurium, *Int. Immunopharmacol.* 11 (2011) 149–156, <https://doi.org/10.1016/j.intimp.2010.10.019>.
- [12] A. Plaper, M. Golob, I. Hafner, M. Oblak, T. Šolmajer, R. Jerala, Characterization of quercetin binding site on DNA gyrase, *Biochem. Biophys. Res. Commun.* 306 (2003) 530–536, [https://doi.org/10.1016/S0006-291X\(03\)01006-4](https://doi.org/10.1016/S0006-291X(03)01006-4).
- [13] W. Wang, G.I.N. Waterhouse, D. Sun-Waterhouse, Co-extrusion encapsulation of canola oil with alginate: effect of quercetin addition to oil core and pectin addition to alginate shell on oil stability, *Food Res. Int.* 54 (2013) 837–851, <https://doi.org/10.1016/j.foodres.2013.08.038>.
- [14] J. Wang, Xi.H. Zhao, Degradation kinetics of fisetin and quercetin in solutions affected by medium pH, temperature and co-existing proteins, *Journal of the Serbian Chemical Society.* 81 (2016) 243–253. <https://doi.org/10.2298/JSC150706092W>
- [15] M.H. Abraham, W.E. Acree, On the solubility of quercetin, *J. Mol. Liq.* 197 (2014) 157–159, <https://doi.org/10.1016/j.molliq.2014.05.006>.
- [16] L. Liu, Y. Tang, C. Gao, Y. Li, S. Chen, T. Xiong, J. Li, M. Du, Z. Gong, H. Chen, L. Liu, P. Yao, Characterization and biodistribution in vivo of quercetin-loaded cationic nanostructured lipid carriers, *Colloids Surf. B: Biointerfaces* 115 (2014) 125–131.
- [17] M. Serhan, M. Sprowls, D. Jackemeyer, M. Long, I.D. Perez, W. Maret, N. Tao, E. Forzani, Total iron measurement in human serum with a smartphone, *AIChE Ann. Meeting. Conf. Proc.* 2019 (Novem 2019) 2012–2014, <https://doi.org/10.1039/x0xx00000x>.
- [18] A. Gray, S. Egan, S. Bakalis, Z. Zhang, Determination of microcapsule physicochemical, structural, and mechanical properties, *Particuology*. 24 (2016) 32–43, <https://doi.org/10.1016/j.partic.2015.06.002>.
- [19] B. Andrade, Z. Song, J. Li, S.C. Zimmerman, J. Cheng, J.S. Moore, K. Harris, J.S. Katz, New frontiers for encapsulation in the chemical industry, *ACS Appl. Mater. Interfaces* 7 (2015) 6359–6368, <https://doi.org/10.1021/acsami.5b00484>.
- [20] K. Essifi, A. Ed-Daoui, D. Berraouan, M. Benelmostafa, M. Dahmani, A. Tahani, Determination of the mechanical properties of single calcium alginate microbeads loaded gallic acid, *Mater. Today: Proc.* 31 (2020) S45–S50, <https://doi.org/10.1016/j.matpr.2020.05.747>.
- [21] B. Lupo, A. Maestro, M. Porras, J.M. Gutiérrez, C. González, Preparation of alginate microspheres by emulsification/internal gelation to encapsulate cocoa polyphenols, *Food Hydrocolloids* 38 (2014) 56–65, <https://doi.org/10.1016/j.foodhyd.2013.11.003>.

- [22] K. Essifi, M. Brahmi, D. Berraouan, A. Ed-Daoui, A. El Bachiri, M.-L. Fauconnier, A. Tahani, J.F. Fernandez-Sanchez, Influence of sodium alginate concentration on microcapsules properties foreseeing the protection and controlled release of bioactive substances, *J. Chem.* 2021 (2021) 1–13, <https://doi.org/10.1155/2021/5531479>.
- [23] K. Essifi, M. Lakrat, D. Berraouan, M.L. Fauconnier, A. El Bachiri, A. Tahani, Optimization of gallic acid encapsulation in calcium alginate microbeads using Box-Behnken Experimental Design, *Polym. Bull.* 78 (2021) 5789–5814, <https://doi.org/10.1007/s00289-020-03397-9>.
- [24] J. Li, S.Y. Kim, X. Chen, H.J. Park, Calcium-alginate beads loaded with gallic acid: preparation and characterization, *LWT - Food Sci. Technol.* 68 (2016) 667–673, <https://doi.org/10.1016/j.lwt.2016.01.012>.
- [25] O. Aarstad, B.L. Strand, L.M. Klepp-Andersen, G. Skjåišk-Bræk, Analysis of G-block distributions and their impact on gel properties of in vitro epimerized mannan, *Biomacromolecules* 14 (2013) 3409–3416, <https://doi.org/10.1021/bm400658k>.
- [26] K. Essifi, M. Lakrat, D. Berraouan, M.-L. Fauconnier, A. El Bachiri, A. Tahani, Optimization of gallic acid encapsulation in calcium alginate microbeads using Box-Behnken Experimental Design, *Polym. Bull.* 78 (10) (2021) 5789–5814, <https://doi.org/10.1007/s00289-020-03397-9>.
- [27] D. Berraouan, M. Elmiz, S. Salhi, A. Tahani, Effect of calcium chloride on rheological behavior of sodium alginate, *Adv. Mater. Proc.* 2 (2017) 629–633, <https://doi.org/10.5185/amp.2017/893>.
- [28] M.H.L. Ribeiro, C. Afonso, H.J. Vila-Real, A.J. Alfaia, L. Ferreira, Contribution of response surface methodology to the modeling of naringin hydrolysis by naringinase Ca-alginate beads under high pressure, *LWT - Food Sci. Technol.* 43 (2010) 482–487, <https://doi.org/10.1016/j.lwt.2009.09.015>.
- [29] A. Shilpa, S.S. Agrawal, A.R. Ray, Controlled delivery of drugs from alginate matrix, *J. Macromol. Sci. - Polym. Rev.* 43 (2003) 187–221, <https://doi.org/10.1081/MC-120020160>.
- [30] B. Zeeb, A.H. Saberi, J. Weiss, D.J. McClements, Formation and characterization of filled hydrogel beads based on calcium alginate: Factors influencing nanoemulsion retention and release, *Food Hydrocolloids* 50 (2015) 27–36, <https://doi.org/10.1016/j.foodhyd.2015.02.041>.
- [31] R.I. Ilescu, E. Andronescu, C.D. Ghitulica, G. Voicu, A. Ficai, M. Hoteteu, Montmorillonite-alginate nanocomposite as a drug delivery system - incorporation and in vitro release of irinotecan, *Int. J. Pharm.* 463 (2014) 184–192, <https://doi.org/10.1016/j.ijpharm.2013.08.043>.
- [32] B.D. Kevadiya, G.V. Joshi, H.A. Patel, P.G. Ingole, H.M. Mody, H.C. Bajaj, Montmorillonite-Alginate nanocomposites as a drug delivery system: Intercalation and in vitro release of vitamin B1 and vitamin B 6, *J. Biomater. Appl.* 25 (2010) 161–177, <https://doi.org/10.1177/0885328209344003>.
- [33] C. Viseras, C. Aguzzi, P. Cerezo, M.C. Bedmar, Biopolymer - clay nanocomposites for controlled drug delivery, 24 (2008). <https://doi.org/10.1179/174328408X341708>
- [34] M. Andersson Trojer, L. Nordstierna, M. Nordin, M. Nydén, K. Holmberg, Encapsulation of actives for sustained release, *PCCP* 15 (2013) 17727–17741, <https://doi.org/10.1039/c3cp52686k>.
- [35] S. Ko, S. Gunasekaran, Controlled release of food ingredients, *Nano-Microencapsul. Foods* (2014) 325–343, <https://doi.org/10.1002/9781118292327.ch13>.
- [36] D.J. McClements, Encapsulation, protection, and delivery of bioactive proteins and peptides using nanoparticle and microparticle systems: a review, *Adv. Colloid Interface Sci.* 253 (2018) 1–22, <https://doi.org/10.1016/j.cis.2018.02.002>.
- [37] D.J. McClements, Encapsulation, protection, and release of hydrophilic active components: potential and limitations of colloidal delivery systems, *Adv. Colloid Interface Sci.* 219 (2015) 27–53, <https://doi.org/10.1016/j.cis.2015.02.002>.
- [38] A. Matalanis, O. Grif, D.J. McClements, Food Hydrocolloids Structured biopolymer-based delivery systems for encapsulation, protection, and release of lipophilic compounds, 25 (2011). <https://doi.org/10.1016/j.foodhyd.2011.04.014>
- [39] D. McClements, Particle characteristics and their impact on physicochemical properties of delivery systems, *Nanopart.- Micropart.-Based Deliv. Syst.* (2014) 79–122, <https://doi.org/10.1201/b17280-4>.
- [40] M. El Miz, H. Akichoh, D. Berraouan, S. Salhi, A. Tahani, Chemical and physical characterization of Moroccan bentonite taken from Nador (North of Morocco), *Am. J. Chem.* 2017 (2017) 105–112, <https://doi.org/10.5923/j.chemistry.20170704.01>.
- [41] K. Essifi, M. Nor, D. Berraouan, E.H. Akichouh, A. El Bachiri, A. Challioui, A. Tahani, Identification and quantification of the adsorption mechanisms of the cationic surfactant the cetylpyridinium chloride on Moroccan Namontmorillonite, *Moroccan J. Chem.* 9 (2021) 142–155, <https://doi.org/10.48317/IMIST.PRSM/morjchem-v9i1.18310>.
- [42] D. Samaha, R. Shehayeb, S. Kyriacos, Modeling and comparison of dissolution profiles of diltiazem modified-release formulations, *Dissolut. Technol.* 16 (2009) 41–46, <https://doi.org/10.14227/DT160209P41>.
- [43] P.L. Ritger, N.A. Peppas, A simple equation for description of solute release I. Fickian and non-fickian release from non-swelling devices in the form of slabs, spheres, cylinders or discs, *J. Control. Release.* 5 (1987) 23–36, [https://doi.org/10.1016/0168-3659\(87\)90034-4](https://doi.org/10.1016/0168-3659(87)90034-4).
- [44] Y. Qi, M. Jiang, Y.L. Cui, L. Zhao, X. Zhou, Synthesis of quercetin loaded nanoparticles based on alginate for Pb(II) adsorption in aqueous solution, *Nanoscale Res. Lett.* 10 (2015) 1–9, <https://doi.org/10.1186/s11671-015-1117-7>.
- [45] X.u. Wang, H. Xie, C. Shi, P. Dziugan, H. Zhao, B. Zhang, Fabrication and characterization of gel beads of whey isolate protein-pectin complex for loading quercetin and their digestion release, *Gels* 8 (1) (2022) 18.
- [46] O.D. Frenç, N. Duteanu, A.C. Teusdea, S. Ciocan, L. Vicaș, T. Jurca, M. Muresan, A. Pallag, P. Ianasi, E. Marian, Preparation and characterization of chitosan-alginate microspheres loaded with quercetin, *Polymers* 14 (3) (2022) 490.
- [47] J.d.L. Souza, C.G. Chiaregato, R. Faez, Green composite based on PHB and montmorillonite for KNO<sub>3</sub> and NPK delivery system, *J. Polym. Environ.* 26 (2) (2018) 670–679.
- [48] S. Dash, P.N. Murthy, L. Nath, P. Chowdhury, Kinetic modeling on drug release from controlled drug delivery systems, *Acta Poloniae Pharm. - Drug Res.* 67 (2010) 217–223.